

Forced Hydrolysis of $\text{In}(\text{OH})_3$ —Comparison of Model with Experiments

Yu Chen, Terry A. Ring
Department of Chemical Engineering
University of Utah
Salt Lake City, Utah 84122

Abstract

This paper presents a theory that links solution complexation equilibria with a model for precipitation predicting the particle size distribution. This model uses classical nucleation theory and growth rates by various rate limiting steps for the growth of the crystals. This model is compared to forced hydrolysis experiments where dilute Indium nitrate solutions, acidified with nitric acid, were heated to 80°C. The experiments produced cubic particles of Indium hydroxide. The experiments were monitored for temperature, pH, turbidity, indium concentration in solution and particle size distribution, all as a function of time for comparison with this model. The model gives an accurate prediction of the evolution of the particle size distribution, pH, turbidity, and indium concentration with time.

Introduction

Forced hydrolysis is a common way to produce metal hydroxides from an acidified metal salt solution. To induce precipitation, this acidified metal salt solution, initially below its solubility and stable with respect to precipitation, is heated to an elevated temperature. Upon heating the solution, the concentration of OH^- ion increases forcing the precipitation of a metal hydroxide. Professor Matijevic has taught us that these metal hydroxides can be precipitated under controlled conditions as monodisperse colloids and as such are of interest for many applications including ceramic powders, magnetic media, imaging materials, toners and pigments. Professor Matijevic¹, over his long and productive career, has been able to produce monodisperse hydroxides of nearly all the metals in the periodic table. Over the years, his work has been expanded by many researchers around the world to produce numerous types of monodisperse particles for numerous new technologies.

In this work, we develop a model of forced hydrolysis which predicts both the particle size distribution of the precipitated particles caused by changes in the concentration of ions in solution. This is done by performing a mass balance on the species in solution that precipitate and using these concentrations to predict the concentration of the other ions in solution, assuming that the solution is in equilibrium with respect to all other species. The results of this model are compared to the experimental system^{2,3,4} where a dilute $\text{In}(\text{NO}_3)_3$ solution acidified with HNO_3 is heated from room temperature to 80°C in a water

bath causing the precipitation of cubic submicron $\text{In}(\text{OH})_3(\text{s})$. This experimental system was chosen because it is simple due to 1) a reduced suite of ion complexes and 2) the precipitation of a crystal with a known geometry. However, the model can be applied to all forced hydrolysis systems.

Mass balances are performed for the Indium metal ions, M^{+m} , and OH^- ions and are given by the generalized differential equations given below :

$$\begin{aligned} \frac{d(\text{OH}^-)}{dt} = & \{ \text{release of OH}^- \text{ from dissociation of H}_2\text{O} \} \\ & - \{ \text{Loss of OH}^- \text{ due to complexation with metal} \} \\ & - \{ \text{Loss of OH}^- \text{ due to nucleation} \} \\ & - \{ \text{Loss of OH}^- \text{ due to crystal growth} \} \end{aligned} \quad (1)$$

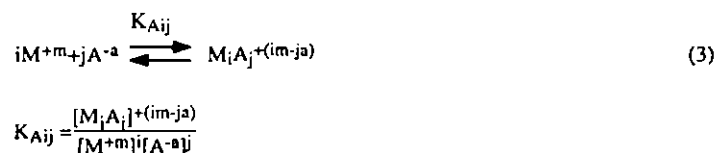
$$\begin{aligned} \frac{d(\text{M}^{+m})}{dt} = & - \{ \text{Loss of M}^{+m} \text{ due to complexation with various anions in solution} \} \\ & - \{ \text{Loss of M}^{+m} \text{ due to nucleation} \} \\ & - \{ \text{Loss of M}^{+m} \text{ due to crystal growth} \} \end{aligned} \quad (2)$$

where [] symbolizes concentration. The initial conditions for these differential equations are: $[\text{OH}^-] = C_2$, at $t = 0$, $[\text{M}^{+m}] = C_3$ at $t = 0$ and $[\text{H}^+] = C_1$ at all time.

All C_i values are constants. Since we are in dilute solution, we will assume that activity and concentration are equivalent. This is not totally accurate. However, to add activity coefficients, which are a function of the ionic strength, and their calculation to these two non-linear coupled differential equations would render them much more time consuming to evaluate. Each of the terms of the above differential equations is discussed below after a discussion of the reactions that take place as an acidified metal salt solution is heated. To resolve these two coupled differential equations, a forward difference technique was used for the time derivatives. This finite difference technique was found to be stable if time steps less than 1 sec. were used.

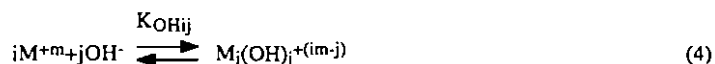
Metal Complexation in Solution

Solution speciation reactions with anions $\text{A} [= \text{NO}_3]$ are given by :



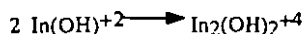
For this work, we will use the NO_3 complexes consisting of $i:j$ equal to 1:1 and 1:2⁵. For these complexes, we have the equilibrium constant, K_{NO_3ij} , and the ΔH_{NO_3ij} of reaction⁶ given in Table 1.

Solution speciation reactions with OH^- ions⁷ also occur in solution :



$$K_{\text{OH}ij} = \frac{[\text{M}_i(\text{OH})_j]^{+(im-j)}}{[\text{M}^{+m}]^i [\text{OH}^-]^j}$$

For this work, we will use Biedermann's model^{8,9} of solution speciation of Indium hydroxide complexes. These include complexes $i:j$, 1:1, 1:2, 2:2, 3:4. These solution complexes have been observed by Raman Spectroscopy^{10,11}. For these complexes, we have the equilibrium constant, $K_{\text{OH}ij}$, and the $\Delta H_{\text{OH}ij}$ of reaction¹² given in Table 1. The reaction kinetics between the 1:1 and the 2:2 complexes have been studied by temperature jump experiments¹³.



The forward rate constant for this reaction was found to be $4.1 \pm 0.4 \times 10^5 \text{ M}^{-1} \text{ sec}^{-1}$. Thus this reaction is fast, occurring within a msec for the solution concentration typically used in forced hydrolysis. Other forward and backward reactions given in equation (4) have not been studied as to their reaction rates as evidence of the lack of information in the literature. In general, other solution speciation reactions can take place with other anions (or cations) B :



$$K_{\text{B}ij} = \frac{[\text{M}_i\text{B}_j]^{+(im-jb)}}{[\text{M}^{+m}]^i [\text{B}^{-b}]^j}$$

However, in this experimental system, there are no other ions in solution for the metal to complex with, but this not always the case in forced hydrolysis. Solution speciation reactions with anions A^{-a} , B^{-b} and OH^- lower the concentration of M^{+m} in solution and lower the supersaturation with respect to the metal hydroxide precipitate.

Table 1 Indium complexation reactions - Equilibrium constants.

$\text{Reactions of the type } i\text{M}^{+m} + j\text{OH}^- \xrightleftharpoons{K_{\text{OH}ij}} \text{M}_i(\text{OH})_j^{+(im-j)}$		
ij	$\log(K_{\text{OH}ij})$ @25°C	ΔH (Kcal/mole)
1:1	9.58	-8.2
1:2	19.67	-13.0
2:2	22.78	-16.0
3:4	46.08	--
$\text{Reactions of the type } i\text{M}^{+m} + j\text{NO}_3^- \xrightleftharpoons{K_{\text{NO}_3ij}} \text{M}_i(\text{NO}_3)_j^{+(im-j)}$		
ij	$\log(K_{\text{NO}_3ij})$ @25°C	ΔH (Kcal/mole)
1:1	-0.43	--
1:2	-0.3	--

Acid Dissociation

Acids present in solution dissociate. For nitric acid, used in this example of forced hydrolysis, the reaction is :



$$K_1 = \frac{[\text{HNO}_3]}{[\text{H}^+][\text{NO}_3^-]} = 10^{-1.44} \text{ @ } 25^\circ\text{C} \text{ and } 10^{-1.18} \text{ @ } 70^\circ\text{C}, \Delta H_{K_1} = 3.3 \text{ Kcal/mole}^{14}$$

Water Ionization

Water's ionization equilibrium is also necessary to describe the experimental system :



$$K_w = [\text{H}^+][\text{OH}^-] = 10^{-13.999} \text{ @ } 25^\circ\text{C} \text{ and } 10^{-12.422} \text{ @ } 90^\circ\text{C}^{15,16}$$

In an acidified metal salt solution $[\text{OH}^-]$ is very low. For a solution with a fixed $[\text{H}^+]$, the $[\text{OH}^-]$ is increased by an increase in the temperature of the solution, since the value of K_w increases with temperature.

Model predictions for $[\text{H}^+]$ and $[\text{OH}^-]$ for a 0.00078 M HNO_3 solution at various temperatures between 25°C and 100°C show that the $[\text{OH}^-] = K_w/[\text{H}^+]$ increases from 10^{-11} M to 10^{-9} M while the $[\text{H}^+]$ and $[\text{NO}_3^-]$ do not change by more than 0.4% and 0.04%, respectively, in this temperature range. Furthermore, if we assume that the $[\text{H}^+]$ is constant, the error in $[\text{OH}^-]$ is less than 0.04%. Experiments performed on heating this solution show a pH change of only 0.05 after temperature compensation. This change is similar to the noise level in these experiments. This proves that NO_3^- complexes and $[\text{H}^+]$ do not vary significantly with temperature. We will take advantage of this insignificant change in $[\text{H}^+]$ and $[\text{NO}_3^-]$ as temperature changes to simplify the necessary differential equations for the mass balance, i.e. no balance is necessary for H^+ or for NO_3^- .

Precipitation of Metal Hydroxide

The reaction of a metal hydroxide is given by :



$$K_{sp} = [\text{M}^{+m}][\text{OH}^-]^m.$$

For Indium hydroxide, K_{sp} is $10^{-36.9} \text{ M}^3$ at 25°C and 10^{-44} M^3 at 90°C (predicted value using $\Delta H_{sp} = 24,789 \text{ cal/mole}^{17}$).

The supersaturation ratio, S , is given by :

$$S = \frac{[\text{M}^{+m}][\text{OH}^-]^m}{K_{sp}(T)} \quad (9)$$

The rate of precipitation will dictate the loss rate of OH^- and In^{+3} ions due to the steps of nucleation and growth of the particles, discussed below.

Release of OH^- due to ionization of H_2O

Rate of precipitation is controlled by the release rate of $[\text{OH}^-]$. We will make the assumption that the forward and reverse reactions responsible for the dissociation of H_2O are very fast (msec.) compared to the rate at which heat can be transferred to the solution (min.). Thus the release rate of $[\text{OH}^-]$ is limited by the change in temperature of the solution¹⁸, $\frac{dT}{dt}$:

$$\frac{d[\text{OH}^-]}{dt} = \frac{d\left(\frac{K_w(T)}{[\text{H}^+]_o}\right)}{dT} \frac{dT}{dt} = \frac{K_w(T)}{[\text{H}^+]_o} \left(\frac{\Delta H_w}{R_g T^2} \right) \frac{dT}{dt} \quad (10)$$

assuming that the $[H^+]_0$ is fixed during the forced hydrolysis experiment. Note, R_g is the gas constant. As a result, the release of $[OH^-]$ is controlled by the heating rate, $\frac{dT}{dt}$, of the solution.

The temperature of the solution is altered by placing a 300 ml vessel containing the solution into a water bath. The vessel's contents starts at a constant temperature, T_0 , often room temperature, and is immersed in water with a constant temperature, T_∞ , assumed to be an infinite reservoir. Heat is transferred to the solution by convection (natural or forced) through the walls of the vessel. We will make the assumption that the solution inside the vessel is all the same temperature and that the heat transfer is given by¹⁹:

$$V \rho C_p \frac{dT}{dt} = h_0 (T_\infty - T) A \quad (11)$$

where V is the vessel's volume, ρ is the density and C_p is the heat capacity of the solution in the vessel, A is the surface area of the vessel exposed to the heat reservoir and h_0 is the overall heat transfer coefficient for both the inside and outside boundary layer, as well as, the heat conduction for the glass wall of the vessel. The solution to this heat balance on the solution in the vessel is given by:

$$T = T_\infty + (T_0 - T_\infty) \exp \left[-\left(\frac{h_0 A}{V \rho C_p} \right) t \right]. \quad (12)$$

Vessels filled with the same volume of solution to be used in forced hydrolysis experiments have been subject to heating tests. The temperature in the vessel was measured with a thermocouple as a function of time. A plot of $(T_0 - T_\infty)/(T - T_\infty)$ as a function of time was made and an exponential curve was used as a best fit ($r^2=0.998$). Analysis of the slope gives the parameter group $\left(\frac{h_0 A}{V \rho C_p} \right)$ [$= 0.1838 \text{ min}^{-1}$] which is all that is needed to determine the temperature versus time curve for any initial, T_0 , and bath, T_∞ .

The temperature change is rather slow in the water bath taking more than 5 minutes to reach 80°C . This equation gives a heating rate, $\frac{dT}{dt}$, for the solution in the test tube of:

$$\frac{dT}{dt} = -\left(\frac{h_0 A}{V \rho C_p} \right) (T_0 - T_\infty) \exp \left[-\left(\frac{h_0 A}{V \rho C_p} \right) t \right] \quad (13)$$

This heating rate can be used in the equation describing the release rate of $[OH^-]$, equation (10), completing a theoretical description of the $[OH^-]$ release rate. As a result of the heating rate, the $[OH^-]$ can be calculated if losses due to nucleation and growth are accounted for, as discussed below.

Loss of M^{+m} due to complexation with anions in solution

The heating rate will also release M^{+m} ions due to the altering of the solution speciation equilibria of the metal with A^{-a} and OH^- ions given by²⁰ :

$$\begin{aligned} \frac{d[\text{M}^{+m}]}{dt} = \frac{dT}{dt} & \left(\sum_i \frac{1}{i} \sum_j \frac{\left\{ \frac{\Delta H_{\text{OH}ij}}{R_g T^2} + j \frac{\Delta H_w}{R_g T^2} \right\}}{\frac{1}{K_{\text{OH}ij} [\text{M}^{+m}]^i [\text{OH}^-]^j} + \frac{1}{[\text{M}^{+m}]}} \right) + \\ & \left(\sum_i \frac{1}{i} \sum_j \frac{\left\{ \frac{\Delta H_{\text{A}ij}}{R_g T^2} \right\}}{\frac{1}{K_{\text{A}ij} [\text{M}^{+m}]^i [\text{A}^{-a}]^j} + \frac{1}{[\text{M}^{+m}]}} \right) \end{aligned} \quad (14)$$

where $\frac{dT}{dt}$ is again the heating rate of the solution. This expression assumes that $[\text{A}^{-a}]$ is not dependant upon temperature which is the case if it is an independent ion added with the metal salt used in the initial formulation of the solution and not complexing anything but the metal. Other solution speciation, i.e. $[\text{M}_i \text{B}_j]$ can also be evaluated in the very same way giving additional terms like the $\text{M}_i \text{A}_j$ term. For the Indium hydroxide system under investigation the equilibrium constants and the enthalpies are given in Table 1. Temperature correction of an equilibrium constant was accounted for by :

$$\frac{d \ln K}{dT} = \frac{-\Delta H}{R_g T^2} \quad (15)$$

Loss of $[\text{OH}^-]$ and $[\text{M}^{+m}]$ due to Nucleation

With precipitation, we need a mass balance on $[\text{OH}^-]$ and $[\text{M}^{+m}]$ since they are changing with the formation of a metal hydroxide. The loss of is due to two processes ; nucleation and growth. For nucleation, we have :

$$\frac{d[\text{OH}^-]}{dt} = - \frac{3 \rho}{M_w} J(S,T) R^*(S,T)^3 \quad (16)$$

$$\frac{d[\text{M}^{+m}]}{dt} = - \frac{\rho}{M_w} J(S,T) R^*(S,T)^3 \quad (17)$$

where ρ is the density and M_w is the molecule weight of the solid,

$J[=J_{\max} \exp\left\{-\frac{32 \gamma^3 (\rho/M_w)^2}{(R_g T)^3 (\ln S)^2}\right\}]$ ²¹ is the nucleation rate^{22,23,24} which is a function of time (i.e. S and T are functions of time) and $R^*(S,T)[= \frac{12 \gamma \rho / M_w}{3 R_g T \ln S}]$ is the size of the critical nuclei²⁵, assuming nuclei and crystals are cubic. $R^*(S,T)$ is also a function of time since S and T are functions of time.

Loss of $[\text{OH}^-]$ and $[\text{M}^{+m}]$ due to Crystal Growth

After a crystal is nucleated at time, t , it will continue to grow until the reaction is stopped or the supersaturation decreases to < 1 . The loss of $[\text{OH}^-]$ and $[\text{M}^{+m}]$ due to crystal growth is therefore given by :

$$\frac{d[\text{OH}^-]}{dt} = -\frac{3}{M_w} \int J(S(t), T(t)) dt \Big|_{t_{\text{nucleated}}}^t \int_{t_{\text{nucleated}}}^t R^2 \frac{dR}{dt} dt \quad (18)$$

$$\frac{d[\text{M}^{+m}]}{dt} = -\frac{p}{M_w} \int J(S(t), T(t)) dt \Big|_{t_{\text{nucleated}}}^t \int_{t_{\text{nucleated}}}^t R^2 \frac{dR}{dt} dt \quad (19)$$

where $\frac{dR}{dt}$ is the growth rate of the crystal from the time it is nucleated until time, t . Generally, the growth rate has the form $\frac{dR}{dt} = C f(S) R^n$. Parameters in the various crystal growth rate models²⁶ are given in Table 2. All growth rates are a function of the saturation ratio, S , which is intern a function of time.

Results of Experiments

Experiments similar to those performed by Hamada, et. al.²⁷ and Yuar, et. al.²⁸ giving submicron cubic crystalline $\text{In}(\text{OH})_3$ particles were performed using a solution 4.0×10^{-4} M $\text{In}(\text{NO}_3)_3$ and 4.0×10^{-4} M HNO_3 , $\text{pH}_{\text{initial}} = 2.80 \pm 0.05$. Using chronomal analysis²⁹ on the average particle size, Hamada, et. al.³⁰ found that the growth limited by a poly-surface nucleation mechanism. 300 ml of this solution was prepared and filtered through a $0.2 \mu\text{m}$ membrane filter and let stand for 24 hrs at room temperature ($22.0 \pm 0.5^\circ\text{C}$). This vessel was then placed in a water bath (filled with a ethylene glycol solution to slow evaporation) at $80.0 \pm 0.1^\circ\text{C}$. At various times 20 ml samples were taken and rapidly quenched to room temperature and measured as to their pH, absorbance at $\lambda = 390 \text{ nm}$ and were centrifuged at 700 G and washed repeatedly with distilled water using ultrasonic agitation³¹. The particle size distribution as measured taking a sample on an aluminum stub for observation with a Cambridge Stereoscan 240 Scanning Electron Microscope. An example of the particles produced by this reaction is given in Figure 1. The particle size distribution was measured by automatically counting ≈ 300 particles of different size in the SEM pictures using Image 1.49TM software³². The error of the size distributions³³ measured was less than 5%. The arithmetic mean size and standard deviation were determined from the particle size distribution. A portion of the samples were also extracted with chloroform solution. The total amount of indium ions and the amount of indium in polymeric hydroxide complex form were detected using a pH shift spectroscopic technique pioneered by Hamada, et. al.³⁴ that uses the colored Indium - 8-quinolinol complex for detection.

Table 2 Crystal Growth Rate

$dR/dt = C \cdot f(S) \cdot R^n$				
Growth Mechanism	C	f(S)	n	Ref
Diffusion Bulk	$\hat{V}DC_{eq}$	S-1	-1	40
Mono Surface Nucleation	$\beta_A D d^{-3}$	$\exp[\Delta G_s^*/k_B T]^{\S}$	2	41
Poly Surface Nucleation	$\frac{(Dd/3)}{(N_A C_{eq})^{2/3}}$	$(S-1)^{2/3} \exp[\Delta G_s^*/k_B T]^{\S}$	0	42
Screw Dislocation	$D_s n_{sc} \beta / (y_0^2 \rho)$	$S^2 / S_1 \tanh(S_1/S)^{\S\S}$	0	43
Chemical Reaction	$\eta \hat{V}DC_{eq}$	S-1	-1	-

$$^{\S} \Delta G_s^* = \beta_L^2 \gamma_c^2 d^2 / (1 \beta_A k_B T \ln S)$$

$$^{\S\S} S_1 = (y_0/y_s)S$$

\hat{V} is the molar volume, N_{Av} is Avogadro's number, C_{eq} is the equilibrium concentration, D is the diffusion coefficient, sub-s surface, η is the Damkohler Number, β_A is the area shape factor for surface nuclei, y_0 is the distance between steps, n_{sc} is the equilibrium surface concentration, $\beta = 1 - \sigma_s/S$ is one minus the maximum surface supersaturation divided by the solution supersaturation, ρ is the density.

Experimental data are presented in Figures 2 and 3. The temperature compensated pH (not shown) decreases approximately 0.30 ± 0.15 pH units after the temperature of the solution is raised. The solution absorbance is near zero for nearly one hour then increases from 100 to 250 min. As a result, we can presume that the particles are nucleated rather quickly and they take time to grow to the a size that is sufficiently large to scatter light. (Note, R^* is $\approx 50 \text{ \AA}$ for these values of S and T .) The mean particle size increases from 150 min. to 300 min. with a decreasing rate and the standard deviation of the particle size distribution generally increases with growth time. The fraction of monomeric Indium complexes [defined as all indium complexes in solution except the $i:j = 3:4$ hydroxide complex] decreases with time. The polymeric Indium complexes [defined as the $3:4$ indium hydroxide species] increases to a maximum concentration at 180 min., then decreases to a



Figure 1. Scanning Electron Micrographs of particles produced at 240 min. Bar = 5 μm .

minimum at 250 min. then increases again. The polymeric Indium complexes have a very low concentration at all times and may be subject to errors since the detection limit of this technique is 6×10^{-6} M or a fraction of 0.015. The measured particle size distributions, shown in Figure 3A, show the increasing size and breadth of the particle size distribution as time progresses.

Comparison with Model Calculations

Utilization of this model allows the prediction of the particle size distribution and the values of $[\text{In}^{+3}]$, $[\text{OH}^-]$, S and all of the species of the type $\text{In}_i(\text{OH})_j^{+(im-j)}$ or $\text{In}_i(\text{NO}_3)_j^{+(im-j)}$, shown in Figure 2, 3 and 4. The parameters used in these model calculations are given in Table 3. These result are highly dependent upon 1) the growth model used for calculation 2) the diffusion coefficient, D , used in both the growth rate and the nucleation rate and 3) the interfacial energy, γ , used in the nucleation rate. Changing the growth law alters the shape of the particle size distribution as it matures with time. The diffusion coefficient alters the speed with which the particles are both nucleated and grow. And the interfacial energy independently alters the nucleation rate which as a consequence alters both the number density of particle and the time over which nucleation takes place, i.e. the nuclei size distribution. The growth model which best fit the particle size data (Figure 2B) (and the absorbance data, Figure 2A) is the diffusion limited growth law. Previous

researchers³⁵ using chronomal analysis have found that poly surface nucleation is the rate determining growth step. However, chronomal analysis uses LaMer's concept of a single burst of nucleation followed by a period of growth which our model suggests is not true because nucleation is continuous, broadening the particle size distribution. The model parameters of diffusion coefficient, D [$=5 \times 10^{-8} \text{ cm}^2/\text{sec}$], and interfacial energy, γ [$=105 \text{ erg/cm}^2$], were altered to give the best fit (by eye) of the particle size distributions. The value of interfacial energy was found to be typical of a solid in a liquid^{36,37} and has a great deal of control of the particle size distribution even for small changes, i.e. 1 erg/cm^2 . The value of the diffusion coefficient is much lower than that typical for ions in solution^{38,39}, i.e. $10^{-5} \text{ cm}^2/\text{sec}$. But since the diffusion coefficient for either nucleation or growth is an effective value which must account for 1) counter diffusion, 2) multi-component diffusion, and hydrated indium ion complex diffusion, it may be reasonable to use such a low value. As a result of these values, the absorbance measurements shown in Figure 2A are also well fit by the model. The absorbance data contains information on the number, as well as the size of the particles. According to Rayleigh's law of light scattering, the intensity of light transmitted through a suspension of length, l , is given by :

$$I = I_0 \exp(-N C_{\text{sca}} l) \quad (20)$$

where I_0 is the incident light intensity, N is the number of particles per unit volume and C_{sca} is the cross section for scattering given by :

$$C_{\text{sca}} = \frac{24\pi^3 V^2}{\lambda^4} \left(\frac{m^2 - 1}{m^2 + 2} \right)^2 \quad (21)$$

where V [$=a^3$] is the volume of the particle, λ is the wavelength, m is the relative refractive index of the particle in the medium, water. Since the model predicts well the particle size data and the absorbance data we can infer that the model also predicts the particle number density well. The model results for the standard deviation of the particle size distribution show the same trend as the experimental results but the model results are about 0.05 higher.

In Figure 4, we see the model results of $[\text{In}^{+3}]$ and $[\text{OH}^-]$ as a function of time as the solution is heated from 22° to 80°C . The OH^- concentration increases as the temperature increases. This increase slows as nucleation and growth proceed. The In^{+3} concentration decreases monotonically as nucleation and growth proceeds. Since $S = \frac{[\text{In}^{+3}][\text{OH}^-]^3}{K_{\text{sp}}}$, we can see that changes in $[\text{In}^{+3}]$ and $[\text{OH}^-]$ impact the driving force, S . S (not shown) increases from ≈ 1 to $\approx 10,000$ as the temperature increases to 80°C and remains high for time $>20 \text{ min}$. until the end of the experiment allowing growth to proceed for several hours at a very high supersaturation. The particles are nucleated over a specific period of time

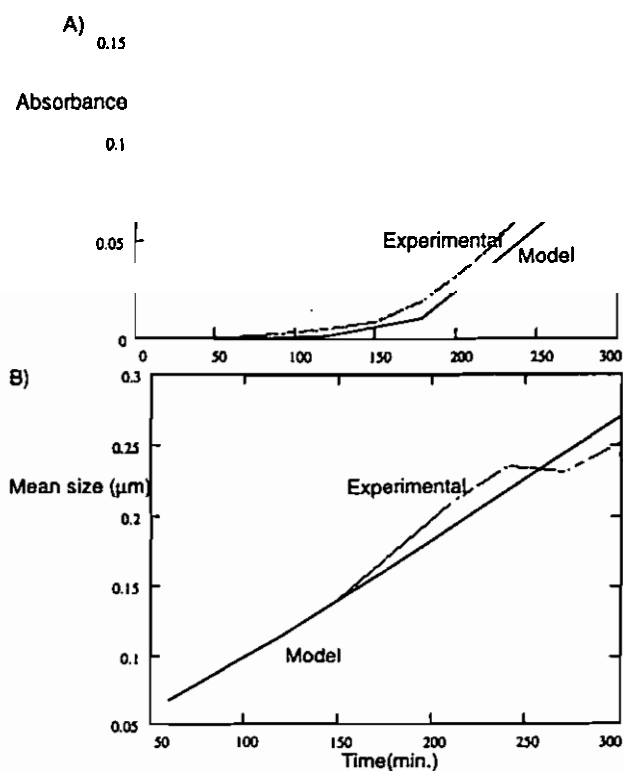


Figure 2. Plot of experimental data for an experiment performed with a $4.0 \times 10^{-4} \text{M}$ $\text{In}(\text{NO}_3)_3$, $4.0 \times 10^{-4} \text{M}$ HNO_3 , $\text{pH}=2.80$, A) Absorbance at $\lambda=390\text{nm}$ (1 cm cell) versus time, B) Mean size and C) Standard Deviation of particle size distributions versus time D) Fraction of monomeric and polymeric Indium species in solution. The sum of solid plus monomeric and polymeric species totals 1.0.

(10 min. $>t_{\text{nucleation}} > 20$ min.) giving a distribution of nuclei sizes which continues to grow as shown in Figure 3. Separate calculations show that the critical value of S is $\approx 10,000$ thus nucleation will be insignificant for all values of $S \ll 10,000$ before the peak in S at ≈ 10 min. The number of particles per unit volume and the particle size as a function of time when compared to experimental values are reasonably accurate, compare Figures 3A and 3B, except for times greater than 250 min when the particle settle out of the reaction vessel.

The way this model has been formulated gives the ability to predict the changes in the concentration of solution species as the experiment proceeds. This is also shown in Figure

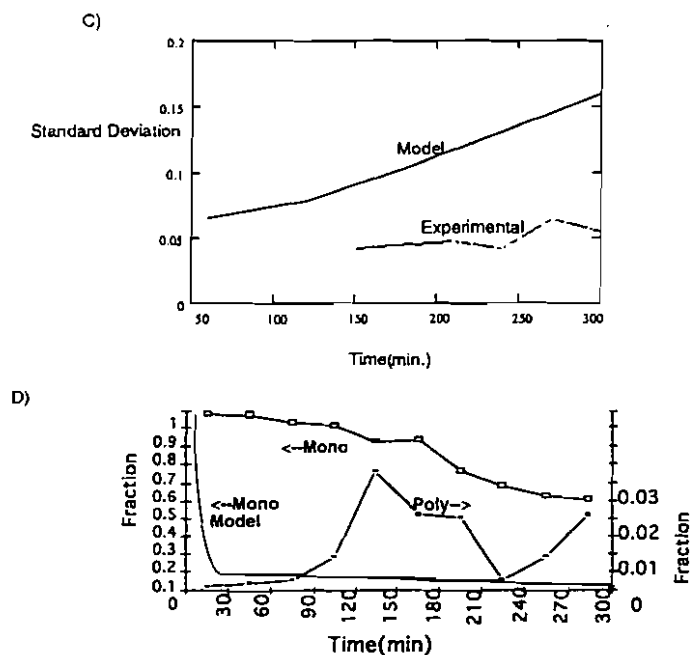


Figure 2. Continued

4. Here we see that the various $[\text{OH}^-]$ complexes initially increase in concentration due to an increase in $[\text{OH}^-]$ and then decrease in concentration as nucleation and growth proceed. The concentration of $[\text{In}^{+3}]$ and the $\text{In}_i(\text{NO}_3)_j$ complexes decrease monotonically. The experimental results for the monomeric and polymeric Indium hydroxide complexes are shown in Figure 2D. Comparing the model and experiment for the monomeric Indium species shows that the model significantly under estimates, however, the downward trend is consistent with experiment. Comparing the model (Figure 4) and experiment (Figure 2D, 3:4 complex) for the polymeric Indium species shows that the model is in significant error, if we can trust the experimental data, as discussed above. Overall the model works well for the number and size distribution of particles produced but does not accurately predict the temporal changes in the monomeric and polymeric Indium species.

Differences between experimental and model results are caused by both experimental problems and model inaccuracies. In experiments, the big particles settling on the bottom or sticking on the glass wall while small particles are lost due to the washing/centrifugation method employed. These experimental problems are observed

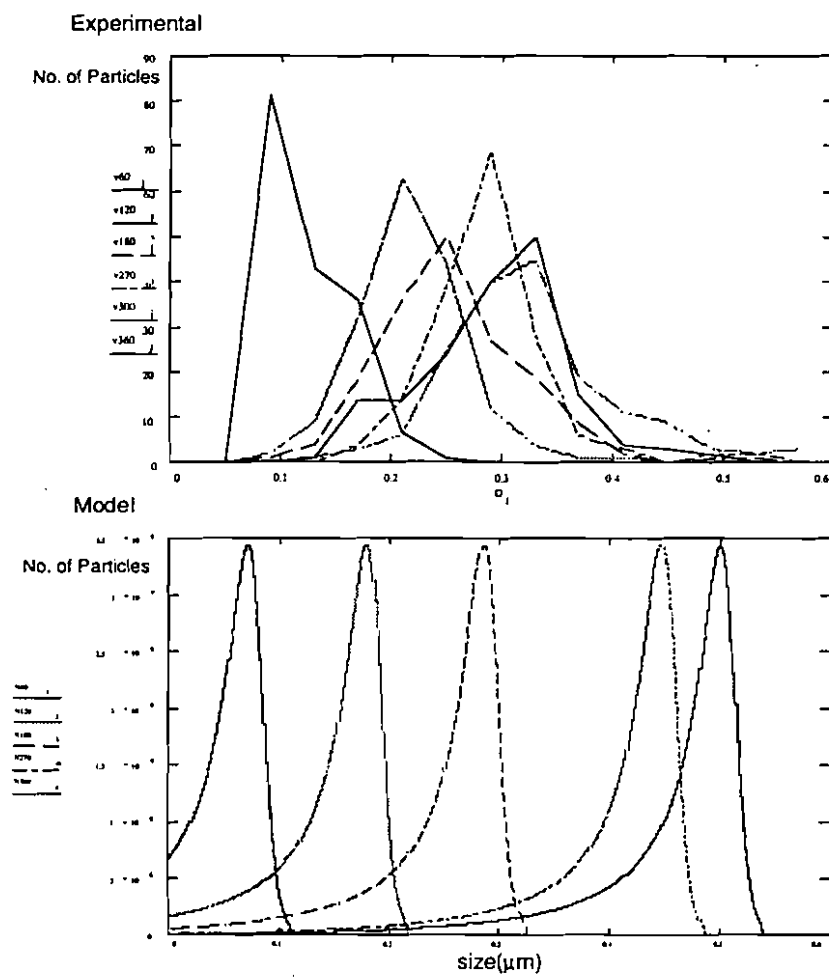


Figure 3. Particle size distributions at various times $v60=60$ min., $v120=120$ min., etc. A) Experimental results B) Model results.

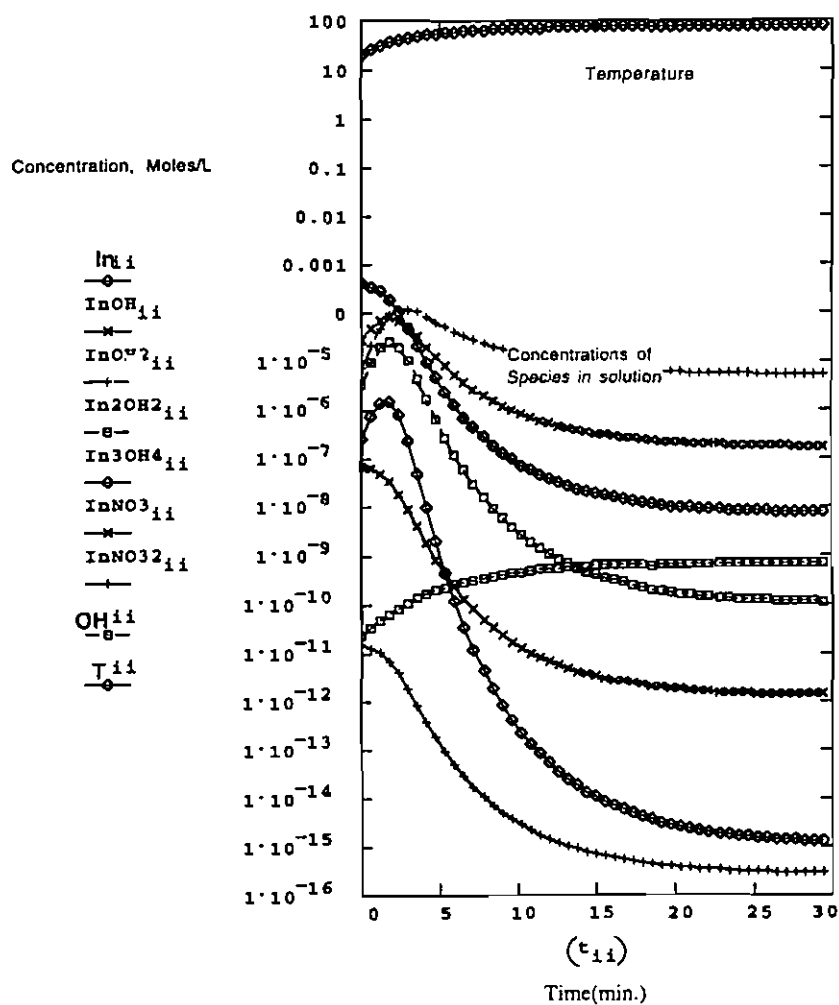


Fig. 4. Concentration of solution species versus time of the forced hydrolysis of $4 \times 10^{-4} \text{M}$ $\text{In}(\text{NO}_3)_3$, $4 \times 10^{-4} \text{M}$ HNO_3 . Using homogeneous nucleation and diffusion limited growth model.

Table 3 Parameters in Model calculation with homogeneous nucleation and the diffusion limited growth law

Parameter	Value	Where Obtained
$\frac{h_0 A}{V \rho C_p}$	0.1838 min ⁻¹	measured
ρ_B	0.04 mole/ cm ³	44
v	0.075 l/ mole	45
D	5x10 ⁻⁸ cm ² /s	Best Fit
γ	105 erg/cm ²	Best Fit
d	5.002x10 ⁻⁸ cm	46
H_w	-13340 cal/ mole	47
K_w	10 ^{-13.99} @ 25°C	-
H_{sp}	24789 cal/ mole	48
K_{sp}	10 ^{-36.9} M ³ @ 25°C	-
$\Delta H_{OHij}, KOH_{ij}$	See Table 1	
$\Delta H_{NO3ij}, KNO3_{ij}$	See Table 1	
ΔH_1	3.30 kcal/ mole	49
K_1	10 ^{-1.18} @ 25°C	-

late in the reaction time. The model doesn't consider the effect of the dissolution of the small particles during quenching, washing and centrifugation on the standard deviation and the resulting change of polymeric indium species in solution. To improve the model, the dissolution of the small particles at late reaction times should be considered. Different values for the model parameters, i.e. the diffusion coefficient and the interfacial energy, should also be considered to better tailor the model so that it will better fit the experimental results.

Conclusions

The hydrolysis of acidified In(NO₃)₃ solution has been studied experimentally. The result is a relatively narrow size distribution of submicron cubic In(OH)₃ crystals. A model of forced hydrolysis has been developed. This model accounts for the varying

concentration of ions in solution as the precipitation proceeds and predicts the particle size distribution. It assumes that all chemical reactions in solution are fast compared to the change in solution temperature. The formalism of this model is a mass balance on both the metal, In^{+3} , and hydroxide, OH^- , ions in solution which allows calculation at any time of the supersaturation ratio, S , the driving force for precipitation. Various crystal growth laws can be incorporated into the model. Comparison between model and experiment shows 1) good agreement of the evolution of the particle size distribution, distribution width and light absorbance with time, 2) reasonable agreement of the indium concentration in solution as a function of time and 3) poor agreement of the indium polymer concentration in solution as a function of time. The richness of data provided by this model gives valuable insight into the details of changes in solution complexation that are responsible for precipitation of monodisperse particles in forced hydrolysis systems.

Acknowledgements

This work is part of the Chemical Engineering M. S. thesis of Yu Chen at the University of Utah.

Endnotes

¹Distinguished University Professor, Dept. Chemistry, Clarkson University, Potsdam, New York.

²Hamada, S. Kudo, Y., and Minagawa, K. Bull. Chem. Soc. Japan 63,102-107(1990).

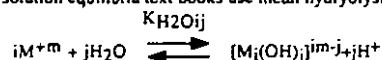
³Yura, K., Fredrikson, K.C. and Matijevic, E., Colloids Surf. 50,281-293(1990).

⁴Yuar, E., and Matijevic, E., J. Colloid Interface Sci.in press.

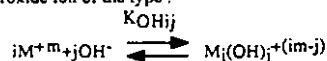
⁵Ferguson, R.C., Doubud, P. and Tuck, D.G., J. Chem. Soc. (A) 1968, 1058.

⁶Smith, R.M. and Martell, A.E., "Critical Stability Constants," Vol.4, Inorganic Complexes, Plenum Press, New York, 1976.

⁷Some solution equilibria text books use metal hydrolysis equilibria of the type :



To generate the $[\text{M}_i(\text{OH})_j]^{im-j}$ ions. This type of equilibria can be converted to solution speciation reactions with the hydroxide ion of the type :



by dividing the hydrolysis equilibrium constant by the water dissociation equilibrium constant raised to the j power, as follows :

$$K_{\text{OH}ij} = \frac{K_{\text{H}_2\text{O}ij}}{K_w^j}$$

⁸Biedermann, G., Ark. Kemi., 9,277(1956), and Rec. Trav. Chim., 75,716(1956).

⁹Biedermann, G. and Ferri, D. Acta Chemica Scandinavica A 36,611-22(1982).

¹⁰Kozhevnikova, G.V. and Keresztury, G., Inorganica Chimica Acta, 98,59-65(1985).

¹¹Hester, R.E., Plane, R.A. and Walrafen, G.A., J. Chem. Phys., 38249(1963).

¹²Smith, R.M. and Martel, A.E., "Critical Stability Constants," Vol.4, Inorganic Complexes, Plenum Press, New York, 1976.

¹³Eyring, E.M. and Owen, J.D., J. Phys. Chem.74(9),1825,10970.

¹⁴Sillen, L.G. and Martel, A.E., "Stability Constants of Metal-ion Complexes," 2 nd. ed., Speciation publication, Chemical Society (Great Britain), No.17, London Chemical Society, 1964.

¹⁵Sillen, L.G. and Martel, A.E., "Stability Constants of Metal-ion Complexes," 2 nd. ed., Speciation publication, Chemical Society (Great Britain), No.17, London Chemical Society, 1964.

¹⁶ $\Delta H_w(\text{cal/mole}) = -2,6613 + 44.487 \cdot T(\text{K}) = -13.34 \text{ Kcal/mole} @ 25^\circ\text{C}^{16}$.

¹⁷determined from a Ksp vs 1/T fit of data from : Lacrois, S., Ann. Chim(France), 4,5(1949), Moeljoer, T., J. Amer. Chem. Soc., 63,2625(1941) and Feitknecht, W. and Schindler, P. Pure Appl. Chem., 6,130(1963).

¹⁸This result was obtained by taking the log of the relationship $[\text{OH}^-] = \frac{K_w(T)}{[\text{H}^+]_0}$ then taking the temperature derivative of both the right and left hand sides, where $[\text{H}^+]_0$ is a constant. Using the relationship

$$\frac{d \ln K_w(T)}{dT} = \frac{-\Delta H}{RgT^2} \text{ and then expanding the term on the left handside } \frac{d \ln [\text{OH}^-]}{dT} \text{ to } \frac{[\text{H}^+]_0}{K_w(T)} \frac{d(\text{OH}^-)}{dT} \text{ and rearranging.}$$

¹⁹Bird, R.B., Stewart, W.E., Lightfoot, E.N., "Transport Phenomenon", John Wiley & Sons, New York, 1960.

²⁰This first summation was obtained by rearranging the equilibrium expression to :

$$[\text{M}_i\text{OH}_j]^{(im-j)} = K_{OHij} [\text{M}^{+m}]^i [\text{OH}^-]^j$$

and taking the derivative with respect to temperature and noting that $\frac{d K_{OHij}}{dT} = K_{OHij} \left\{ \frac{-\Delta H_{OHij}}{RgT^2} \right\}$

and that $\frac{d \{[\text{M}_i\text{OH}_j]^{(im-j)}\}}{dT} = -i \frac{d \{[\text{M}^{+m}]\}}{dT}$ and then rearranging using expressions in ref. 28.

²¹Jmax for aqueous solution is either 10^{33} or $10^{30} \text{ #/cm}^3/\text{sec}$ depending upon the theory used, see ref. 36.

²²Becker, R. and Doring, W., Ann. Physik, 24, 719-752,(1935).

²³Volmer, M. and Weber, A., Z. Phys. Chem. 119,227,(1926).

²⁴Nielsen, A.E., Kinetics of Precipitation, Pergamon Press, Oxford, (1964).

²⁵Nielsen, A.E., Kinetics of Precipitation, Pergamon Press, Oxford, (1964).

²⁶Dirksen, J.A. and Ring, T.A., Chem. Eng. Sci. 46(10),2389-2427(1991).

²⁷Hamada, S., Kudo, Y. and Minagawa, K., Bulletin of the Chemical Society of Japan, 63(1),102-107(1990).

²⁸Yura, K., Fredrikson, K.C. and Matijevic, E., Colloids Surf. 50,281-293(1990).

²⁹Nielsen, A.E., Kinetics of Precipitation, Pergamon Press, Oxford, (1964).

³⁰Hamada, S., Kudo, Y. and Minagawa, K., Bulletin of the Chemical Society of Japan, 63(1),102-107(1990).

³¹Branson 3200 ultrasonic bath.

³²Public domain software developed by National Institutes of Health.

³³Ring, T.A., "Fundamentals of Ceramic Powder Processing and Synthesis", Academic Press, Boston, 1996, p. 56.

³⁴Hamada, S., Kudo, Y., and Minagawa, K. Bull. Chem. Soc. Japan 63,102-107(1990).

³⁵Hamada, S., Kudo, Y., and Minagawa, K. Bull. Chem. Soc. Japan 63,102-107(1990).

³⁶Nielsen, A.E., Kinetics of Precipitation, Pergamon Press, Oxford, (1964).

³⁷McColm, I. J. and Clark, N. J., "Forming, Sharping, and Working of high performance ceramics", p.19, Blackie; New York : Chapman and Hall, 1988.

³⁸R. B. Bird, W. E. Stewart and E. N. Lightfoot, "Transport Phenomena", John Wiley & Sons, 1960.

³⁹R. H. Perry and Don Green, "Perry's Chemical Engineers' Handbook", 6th ed, Mc Graw Hill.

⁴⁰Volmer, M.M. "Kinetik der Phasenbildung" p.209 Steinkopff, Dresden, Leipzig, 1939.

⁴¹Nielsen, A.E., Kinetics of Precipitation, Pergamon Press, Oxford, (1964).

⁴²ibid

⁴³Elwell, D. and Scheel, H.J. "Crystal Growth from High-Temperature Solution", Academic Press Inc., London, 1975.

$$^{44} p\beta = 3 \times \frac{2.2 - \frac{8}{\text{cm}^3}}{165.84 - \frac{8}{\text{mole}}}$$

$$^{45} \text{Molar volume, } v = \frac{165.84}{2.2 \times 1000}$$

⁴⁶The size of molecule, $d = \left(\frac{165.84}{N_{\text{av}} \times 2.2} \right)^{1/3}$ cm, assuming the molecular shape is cubic.

⁴⁷ $\Delta H_w(\text{cal/mole}) = -2,6613 + 44.487 \times T(\text{K}) = -13.34 \text{ Kcal/mole @ } 25^\circ\text{C}.$

⁴⁸determined from a K_{sp} vs $1/T$ fit of data from : Lacrois, S., Ann. Chim(France), 4,5(1949), Moellner, T., J. Amer. Chem. Soc., 63,2625(1941) and Feitknecht, W. and Schindler, P. Pure Appl. Chem., 6,130(1963).

⁴⁹Sillen, L.G. and Martell, A.E., "Stability Constants of Metal-ion Complexes," 2nd ed., Speciation publication, Chemical Society (Great Britain), No.17, London Chemical Society, 1964.